

Spin transition of Fe²⁺ in ringwoodite (Mg,Fe)₂SiO₄ at high pressures

IGOR S. LYUBUTIN¹, JUNG-FU LIN², ALEXANDER G. GAVRILIUK^{1,3,*}, ANNA A. MIRONOVICH³, ANNA G. IVANOVA¹, VLADIMIR V. RODDATIS⁴ AND ALEXANDER L. VASILIEV^{1,4}

¹Shubnikov Institute of Crystallography, Russian Academy of Sciences, Moscow 119333, Russia

²Department of Geological Sciences, Jackson School of Geosciences, The University of Texas at Austin, Austin, Texas 78712-0254, U.S.A.

³Institute for Nuclear Research, Russian Academy of Sciences, 60-letiya Oktyabrya prospekt 7a, Moscow 117312, Russia

⁴National Scientific Center, “Kurchatov Institute,” Moscow 123098, Russia

ABSTRACT

Electronic spin transitions of iron in the Earth’s mantle minerals are of great interest to deep-Earth researchers because their effects on the physical and chemical properties of mantle minerals can significantly affect our understanding of the properties of the deep planet. Here we have studied the electronic spin states of iron in ringwoodite (Mg_{0.75}Fe_{0.25})₂SiO₄ using synchrotron Mössbauer spectroscopy in a diamond-anvil cell up to 82 GPa. The starting samples were analyzed extensively using transmission and scanning electron microscopes to investigate nanoscale crystal chemistry and local iron distributions. Analyses of the synchrotron Mössbauer spectra at ambient conditions reveal two non-equivalent iron species, (Fe²⁺)₁ and (Fe²⁺)₂, which can be attributed to octahedral and tetrahedral sites in the cubic spinel structure, respectively. High-pressure Mössbauer measurements show the disappearance of the hyperfine quadrupole splitting (*QS*) of the Fe²⁺ ions in both sites at approximately 45–70 GPa, indicating an electronic high-spin (HS) to low-spin (LS) transition. The spin transition exhibits a continuous crossover nature over a pressure interval of ~25 GPa, and is reversible under decompression. Our results here provide the first experimental evidence for the occurrence of the spin transition in the spinel-structured ringwoodite, a mantle olivine polymorph, at high pressures.

Keywords: Ringwoodite (Mg,Fe)₂SiO₄, high pressure, spin crossover, Mössbauer spectroscopy

INTRODUCTION

Earth’s transition zone is mainly composed of Fe-bearing Mg₂SiO₄ polymorphs. Extensive studies have been devoted to studying their structural stability as well as their physical and chemical properties under relevant pressure-temperature (*P-T*) conditions of the region (e.g., Akimoto and Ida 1966; Ringwood and Major 1966; Suito 1972; Ohtani 1979; Yagi et al. 1974; Morishima et al. 1994; Fei and Bertka 1999; Koch-Müller et al. 2009). Three polymorphs of Fe-bearing Mg₂SiO₄ are widely considered to be potentially present in the upper mantle: (1) olivine [α -(Mg,Fe)₂SiO₄], which occurs abundantly in upper-mantle peridotite; (2) wadsleyite [β -(Mg,Fe)₂SiO₄] with the modified spinel (SPL) structure, which occurs at pressures (*P*) exceeding 13 GPa and temperatures of above ~1000 °C; (3) ringwoodite [γ -(Mg,Fe)₂SiO₄] with the spinel structure (SP), which exists at *P-T* conditions between approximately 520 km (*P* ≈ 17.5 GPa, *T* ≈ 2000 K) and 670 km (*P* ≈ 24 GPa, *T* ≈ 2200 K) in depth. These studies have also shown that wadsleyite is not stable in the Fe₂SiO₄-rich portion of the system in which fayalite (α -Fe₂SiO₄) transforms directly into γ -Fe₂SiO₄ (SP) at ~5.3 GPa and 1000 °C (Frost 2008). On the other hand, Woodland and Angel (1998) have synthesized a phase isostructural to wadsleyite containing a significant amount of Fe³⁺. Their synthesis was performed using a mixture of fayalite and magnetite at 5.6 GPa and 1100 °C. Woodland and Angel (2000) further showed that the Fe₂SiO₄-Fe₃O₄ series consists of three spinel-like polytypes isostructural to modified spinel phases II, III, and V in Ni-Al silicate systems.

Koch et al. (2004) added Mg₂SiO₄ into the Fe₂SiO₄-Fe₃O₄ series and subjected the mixture to between 4 and 9 GPa and 1100 °C, producing three intermediate phases of the modified spinel II, III, and V. They showed that the maximum Mg content in the phase III is limited to 15 mol% Mg₂SiO₄. These previous studies thus indicate a very rich crystal chemistry in the Fe₂SiO₄-Mg₂SiO₄ series as a function of *P-T* and iron content.

Understanding the physics and chemistry of these polymorphs as a function of *P-T* and iron content is of great interest to deep-Earth researchers because such information may help us decipher geophysical and geochemical processes in the Earth’s mantle. These reported structural modifications are based on the cubic close-packed oxygen sublattices that differ in the filling of the interstitial consisting of one tetrahedron and two octahedra. In these structural modifications, the tetrahedrally coordinated Si⁴⁺ ion is partially replaced by Fe³⁺ ion in all these polymorphs while Fe²⁺ is partially replaced by Fe³⁺ to retain the charge balance. Yamanaka et al. (1998, 2001) and van Aken and Woodland (2006) also observed a disordering of Si⁴⁺ between tetrahedral and octahedral sites of the modified spinel V phase, in which 7% of the Si⁴⁺ was found to be in the octahedral site. This type of cation disorder in ferromagnesian silicate spinel has been discussed and reviewed in details by Hazen (1993), Hazen et al. (1993b), and Hazen and Yang (1999).

Pressure-induced electronic spin-pairing transitions of iron and their associated effects on the physical properties of host phases have been recently observed to occur in lower-mantle minerals including ferropericlase, silicate perovskite, and post-perovskite at high *P-T* [e.g., see Lin and Tsuchiya (2008) for a review]. Spe-

* E-mail: gavriliuk@mail.ru

cifically, the spin crossover of Fe²⁺ in ferropericlasite occurs over a wide *P-T* range extending from the middle to the lower section of the lower mantle (Lin et al. 2007; Lyubutin et al. 2009; Mao et al. 2011). Iron is the most abundant 3d transition metal in the Earth's interior; its existence in mantle minerals has been documented to affect a broad spectrum of the minerals' physical and chemical properties (e.g., McCammon 1997, 2006; Irifune et al. 2010). In particular, changes in the spin and valence states of iron as a function of *P-T* have attracted great interest because they can affect physical, chemical, rheological, and transport properties of the lower-mantle minerals (Lyubutin et al. 2013). Previous studies have focused mainly on the spin and valence states of the lower-mantle minerals, whereas our knowledge on the spin and valence states of iron in transition zone minerals, such as ringwoodite, is largely lacking.

Here we present a study of the spin and valence states of iron in transition-zone ringwoodite using synchrotron Mössbauer spectroscopy (SMS) in a diamond-anvil cell (DAC). Due to the complex crystal chemistry of the olivine polymorphs reported previously and mentioned above, we have used several advanced analytical techniques to characterize the starting sample, including energy-dispersive X-ray microanalysis (EDXMA), transmission/scanning electron microscopy (TEM/STEM), and electron diffraction (ED) to help interpret high-pressure Mössbauer results. Our results here are applied to further understand the nature of the spin transition in Earth's mantle minerals at high pressures.

EXPERIMENTAL METHODS

Sample synthesis and characterization

Polycrystalline samples were synthesized in a multi-anvil apparatus using ⁵⁷Fe-enriched starting material [(Mg,Fe)O-SiO₂ mixture] in a Pt capsule at targeted conditions of ~22 GPa and 2000 K; however, the real sample temperature was likely in the ringwoodite stability field (lower temperature than expected). The synthesized sample was extracted from the capsule and extensively analyzed using EDXMA, TEM, ED, and SMS. For the TEM analyses, several cross sections of the sample were prepared by focused ion beam (FIB) milling technique using a Helios dual beam system (FEI, Oregon, U.S.A.), which combines scanning electron microscope and FIB (SEM/FIB) equipped with C and Pt gas injectors and micromanipulator (OmniProbe, Texas, U.S.A.). A Pt layer 2–3 μm thick was deposited on the surface of the sample prior to the cross-section preparation by FIB milling procedure. Cross sections measuring with a surface area of 8 × 5 μm² and a thickness of 0.5 μm were cut by 30 kV Ga⁺ ions, removed from the bulk sample, and then attached to an OmniProbe semi-ring (OmniProbe, Texas, U.S.A.). Final thinning was performed with 30 kV Ga⁺ ions followed by cleaning with 2 keV Ga⁺ ions to allow for the electron transparency in TEM/STEM experiments. All specimens were studied using a transmission/scanning electron microscope Titan 80-300 (FEI, Oregon, U.S.A.) equipped with a spherical aberration (C_s) corrector (electron probe corrector), a high-angle annular dark-field (HAADF) detector, an atmospheric thin-window energy-dispersive X-ray (EDX) spectrometer (Phoenix System, EDAX, Mahwah, New Jersey, U.S.A.), and post-column Gatan energy filter (GIF; Gatan, Pleasanton, California, U.S.A.). The TEM analyses were performed at 300 kV. A RAPID CCD camera was used to record electron diffraction patterns. Since high-pressure synthesized samples were likely sensitive to irradiation of the electron beam, we also used a liquid nitrogen (LN₂) cooled holder (Gatan 636 Double Tilt, Gatan, Pennsylvania, U.S.A.) to prevent potential sample decomposition and/or amorphization during the study (see results for details).

High-pressure synchrotron Mössbauer spectroscopic measurements

Electronic spin and valence states of iron ions in the synthesized sample were studied using SMS technique [also called nuclear forward scattering (NFS)] in a DAC at the 16ID-D sector of the HPCAT Beamline (Sector 16) of the Advanced Photon Source, Argonne National Laboratory (APS, ANL). A double-polished sample platelet with dimensions of approximately 80 × 80 μm² in size and 5 μm in thickness was

loaded into a DAC having 300 mm diamond-anvil culets. The platelet's effective thickness for the SMS experiments was estimated to be around 2–3 based on fitting results of the Mössbauer spectra (Gavriluk et al. 2006). A rhenium gasket with an initial thickness of 250 μm was pre-indented to 30 μm and a hole of 150 μm was drilled into the gasket for use as a sample chamber. To maintain quasi-hydrostatic pressure conditions of the sample chamber, mineral oil was loaded into the sample chamber and used as the pressure medium, together with a few ruby chips that acted as pressure calibrants. Pressure in the sample chamber was determined by the ruby fluorescence method (Mao et al. 1978).

SMS experiments were performed at 16ID-D beamline of the APS, ANL. A high-resolution monochromator with 2.2 meV bandwidth was tuned to nuclear resonance energy of 14.4125 keV for the Mössbauer transition of ⁵⁷Fe in the sample (Shvyd'ko et al. 2000). The synchrotron beam was focused down to ~60 μm (FWHM) by a pair of KB mirrors and further slit down to about 20 μm using a Pt pinhole of 20 μm in diameter drilled in a 200 μm thick Pt disk. This allowed the SMS spectra to be taken from a relatively small area of the sample with a lesser pressure gradient. Based on the experience learned from our numerous previous experiments, mineral oil serves as a quasi-hydrostatic pressure medium with relatively small local stresses in diamond-anvil cell experiments. We also note that we had used several ruby chips across the sample chamber to evaluate pressure gradients from the center to the edge of the chamber. Meanwhile, the SMS spectra were collected from a small region of ~20 μm near the center of the chamber by using a 20 μm pinhole to define the X-ray beam size. Based on these analyses, we believed that the pressure gradient across the region of the measured sample was about 2%. These arguments allow us to state that the conditions of measurements were close to hydrostatic. Synchrotron time spectra of the ⁵⁷Fe nuclei in the sample were recorded by an avalanche photo diode (APD) detector in the forward direction in the pressure range between ambient pressure and 82 GPa during compression and decompression runs. The spectra were evaluated using the MOTIF program (Shvyd'ko 1999) to permit derivation of the hyperfine parameters.

RESULTS

TEM and STEM analyses

Low-magnification bright-field (BF) and HAADF STEM images of the specimen are shown in Figures 1a–1d, respectively. In the upper part of the images of sample 1 (Figs. 1a and 1b), the “hair-like” contrast was a result of the partially-sputtered (by FIB) protective Pt film. These images, together with the image of specimen 2 (Fig. 1c), showed that sample platelet exhibited polycrystalline microstructures consisting of fine grains 0.1–1.5 μm in diameter, separated by minor intercalations (ground matrix). Most grains exhibited irregular faceted morphology, though a few grains had rather circular rounded morphology and were surrounded by nano-cracks. These grains were relatively bright in the STEM images (Figs. 1b and 1c), most likely due to an excess of heavier Fe atoms. Diffraction contrasts of the irregular and rounded particles on the BF TEM images were obtained at higher magnifications (Fig. 1d). The results showed that these grains were single crystals with some internal strain. The minor intercalations, on the other hand, appeared darker in the HAADF STEM images (Figs. 1b and 1c), and could be associated with higher content of light elements including Mg, Si, and O. Energy filtering of the BF images with energy shift 40 ± 5 eV, which was chosen experimentally to obtain the highest contrast possible, showed that the intercalations were approximately 0.01–0.70 μm thick. The intercalations were made of amorphous materials as unambiguously revealed by the analyses of the BF images and further ED studies (Fig. 1d) (see discussion below for details).

Energy-dispersive X-ray microanalysis (EDX microanalysis)

The results of EDX Fe, Si, and Mg element mapping are presented in Figure 2. These measurements showed that the rounded grains were more Fe rich while the ground matrix contained

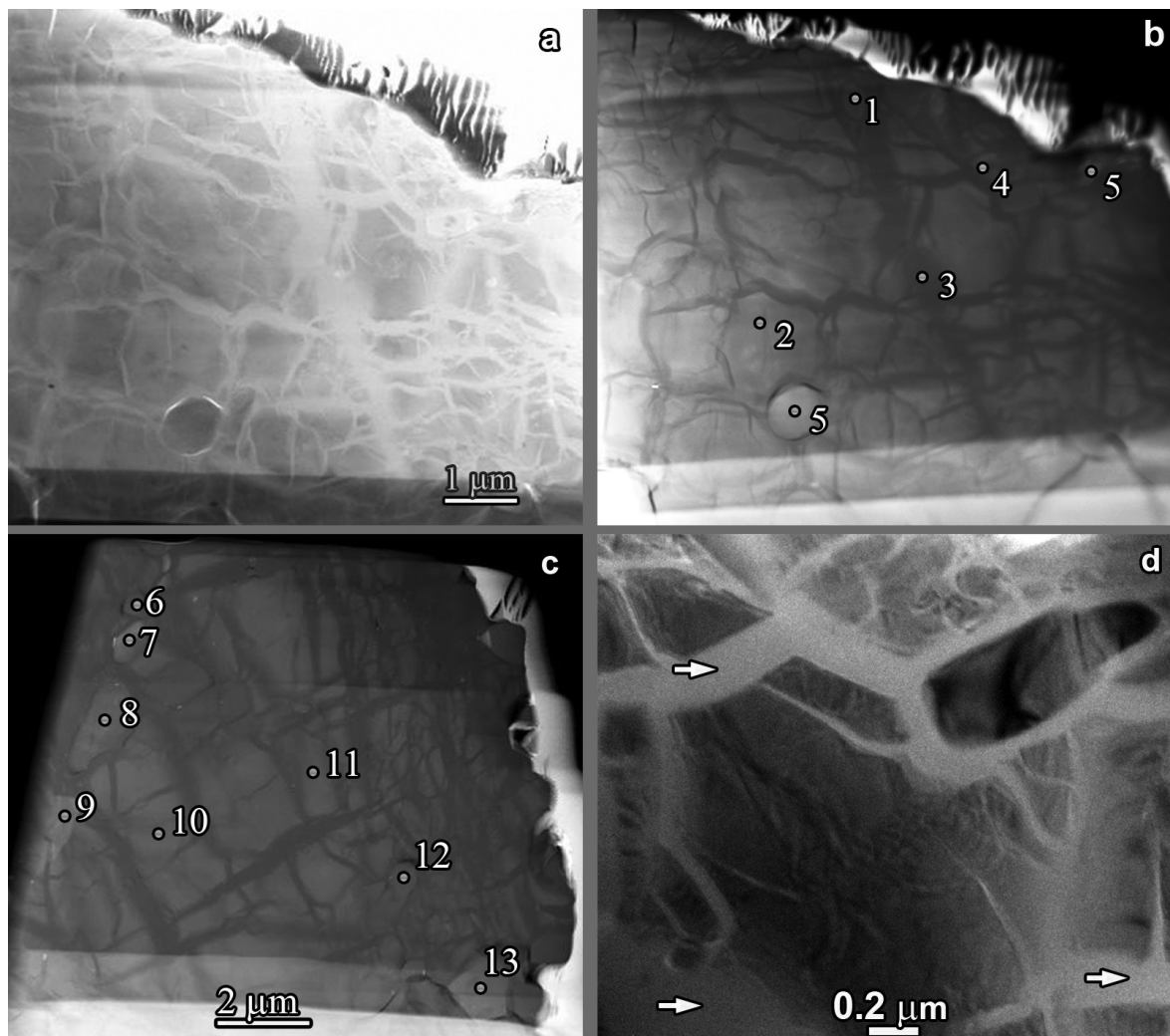


FIGURE 1. The images of the specimens: (a) The BF TEM image of specimen 1. (b) HAADF STEM image of specimen 1. The areas of EDXMA analyses are indicated. (c) HAADF STEM image of specimen 2 with the indicated areas of EDXMA analyses. (d) Enlarged BF TEM image of ringwoodite particle, the amorphous intercalations are shown by white arrows.

more Mg and Si, consistent with the HAADF STEM results. To obtain more accurate statistics, we performed semi-quantitative energy-dispersive X-ray microanalysis (EDXMA) for a number of grains shown in Figures 1b and 1c. The representative EDXMA spectra are shown in Figure 3. We observed lower than expected O element statistics based on proposed stoichiometry, which may be a result of the presence of the uneven specimen surface and e^- beam induced amorphization, together with low-energy X-ray shielding. On the contrary, excess O content was observed in some areas (see for instance no. 4).

The EDXMA data in Figures 1b and 1c and Table 1 indicate that Fe predominantly presents itself in the rounded grains with a chemical formula of $(\text{Mg}_{0.75}\text{Fe}_{0.25})_2\text{SiO}_4$ which is mostly present in the ringwoodite phase (see TEM data below for details), whereas the minor intercalations (a few percent in abundance and mostly $<1 \mu\text{m}$ thick) had a stoichiometry very close to MgSiO_3 with a chemical formula of $(\text{Mg}_{0.95}\text{Fe}_{0.05})\text{SiO}_3$ (as seen, for example, in area no. 3 of Fig. 1b). Representative EDXMA spectra obtained from selected areas of two specimens are shown in Figures 3a–3c.

Since Fe is primarily present in ringwoodite, we conclude that the SMS spectra should not be affected by the presence of minute $(\text{Mg}_{0.95}\text{Fe}_{0.05})\text{SiO}_3$ (see further discussion below).

Electron diffraction (ED) data

To relate the chemical analyses to the crystal structure of the major Fe-rich grains eventually used for Mössbauer measurements, specific grains were further investigated using electron diffraction techniques (Figs. 4a–4c). Analyses of the diffraction patterns using interplanar distances and angles between the diffraction maxima indicate that the crystal structure corresponds to a cubic system with a lattice parameter $a = 8.06 (\pm 0.10) \text{ \AA}$. Moreover, when tilted along the $00l$ Kikuchi band to a position between zone axes, a clear modulation of the reflection patterns appeared while odd reflections disappeared (Fig. 4b). We thus conclude that most of the observed reflections at the zone axis orientations must arise from multiple scattering, i.e., $00l$ reflections with $l \neq 2n$ may also be kinematically forbidden. The additional row of the reflections from which the multiple

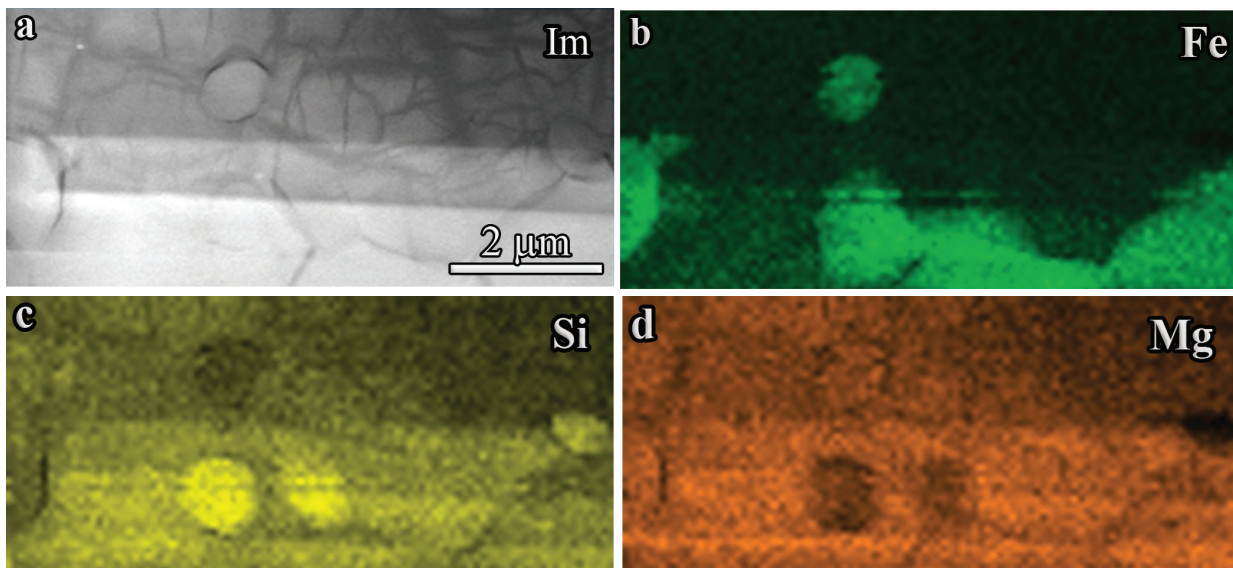


FIGURE 2. (a) HAADF STEM image of the specimen and corresponding element distribution mapping results: (b) Fe; (c) Si; (d) Mg. (Color online.)

scattering occurred was also visible in the selected-area electron diffraction (SAED) pattern. Additional evidence for the space group of the $(\text{Mg}_{0.75}\text{Fe}_{0.25})_2\text{SiO}_4$ phase was obtained by tilting the crystal around the $[\bar{1}11]$ and $[\bar{1}\bar{1}1]$ axes, in which significant decrease in the intensity of the 222 reflections was observed (Fig. 4c). However, we cannot completely rule out the double diffraction effect due to the small distance between the zone axes in reciprocal space.

The systematic absences of reflections are what one would expect for the space group $Fd\bar{3}m$ (Hahn 2006). Further verification of this space group and lattice parameters was performed for another zone axis. The SAED pattern corresponding to the $B = [310]$ zone axis (Fig. 5a) together with the respective Kössel ED pattern in the convergent electron beam were also obtained (Fig. 5b). Converting the radius of the first-order Laue zone (FOLZ) ring to a Laue zone spacing parallel to the beam direction, we obtained an interplanar spacing typical for the structure with the space group $Fd\bar{3}m$ having a lattice parameter of $8.06 (\pm 0.10)$ Å. Based on all of our detailed chemical and structural analyses of the rounded grains, we conclude that the synthesized sample was mainly made of Fe-rich ringwoodite $[(\text{Mg}_{0.75}\text{Fe}_{0.25})_2\text{SiO}_4]$.

Analyses of the ED data obtained from the minor intercalations with approximately $(\text{Mg}_{0.95}\text{Fe}_{0.05})\text{SiO}_3$ (area no. 2 in Fig. 1b) revealed an orthorhombic crystal structure with the space group $Pnma$ and the unit-cell parameters $a = 4.93 (\pm 0.10)$ Å, $b = 6.90 (\pm 0.10)$ Å, and $c = 4.78 (\pm 0.10)$ Å (O’Keeffe et al. 1979), consistent with the structure of the lower-mantle silicate perovskite. A representative SAED pattern obtained for $B = [121]$ zone axis is presented in Figure 6. Possible existence of other phases with different crystal structures, including enstatite (space group $Pbcn$) (Sasaki et al. 1982), clinoenstatite (space group $P12_1/C1$) (Angel et al. 1992), and protoenstatite (space group $Pbcn$) (Murakami et al. 1984), were ruled out based on the analyses of the electron diffraction patterns (Fig. 6). These small particles are extremely unstable under the e^- beam irradiation, and can rapidly degrade to an amorphous state, even with

the use of a LN_2 cooled sample holder. These observations are consistent with the metastable nature of silicate perovskite at ambient conditions reported previously.

High-pressure Mössbauer spectroscopy results

Synchrotron ^{57}Fe -Mössbauer spectra of the sample were collected at high pressures up to 82 GPa (Fig. 7). The starting sample was mostly ringwoodite $[(\text{Mg}_{0.75}\text{Fe}_{0.25})_2\text{SiO}_4]$ based on the aforementioned analyses; however, a small amount of perovskite could have been present in the sample. Nevertheless, it should not affect the overall spectra of ringwoodite, as the amount of perovskite and its 1 at% iron content are negligible as compared to that of the dominant ringwoodite. In general, the damped decay of nuclear excitation is modulated in time by quantum and dynamic beats (Smirnov 1999). The quantum beats are caused by the interference of the scattered radiation components with different frequencies as a result of the ^{57}Fe nuclear level splitting into sublevels due to the hyperfine interaction. The period of quantum beats is inversely proportional to the hyperfine splitting and, in our case here, to the electric quadrupole splitting (QS). The dynamic beats are caused by multiple scattering processes and are controlled by the sample thickness (Smirnov 1999). The observed low-frequency quantum beats indicate that all iron ions are in a paramagnetic state without magnetic ordering at room temperature.

The quantum beats were present in the SMS spectra at pressures up to 45 GPa, underwent significant changes between 35 and 70 GPa, and completely disappeared above 70 GPa. The disappearance of the quadrupole splitting signals an electronic spin transition. The straight-line shape of the nuclear excitation decay observed above 70 GPa indicates an absence of the dynamic beats in our thin sample, which simplifies the spectral fitting procedure without the need to consider the dynamic effects on the spectra (Gavriliuk et al. 2006).

The Mössbauer spectrum at ambient conditions has a quadrupole doublet shape characteristic of the paramagnetic iron state. The thick sample was analyzed by Mössbauer spectroscopy with a

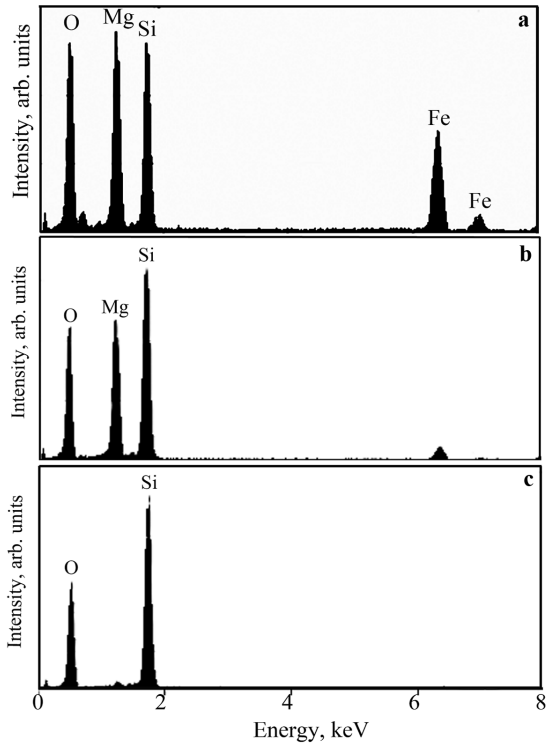


FIGURE 3. Representative EDXMA (energy-dispersive X-ray microanalysis) spectra obtained from areas shown in Figures 1b and 1c: (a) area no. 13, similar to the areas no. 5 and 7; (b) area no. 3 and 10; (c) area no. 6.

laboratory source at ambient conditions. Analyses of the measured Mössbauer spectra showed that 87.8% of the total iron was in the pure Fe²⁺ state (with isomer shift IS = 1.02 mm/s) while 12.8% of the iron was in the Fe²⁺-like state. The value of the isomer shift IS of ~0.69 mm/s is close to that of Fe²⁺, but could also be interpreted as the intermediate state between Fe²⁺ and Fe³⁺ with an averaged

TABLE 1. Results of the EDX microanalysis (in at%) in the areas denoted by corresponding numbers in Figures 1b and 1c (accuracy of the measurements is within 1 at%)

No.	Mg	Fe	Si	O	Compound
1			33	67	SiO ₂
2	21	1	22	56	(Mg,Fe)SiO ₃
3	20	1	20	59	(Mg,Fe)SiO ₃
4	4		23	73	SiO ₂ +H ₂ O
5	21	6	17	56	~(Mg _{0.78} Fe _{0.22}) ₂ SiO ₄
6	1		39	60	SiO ₂
7	21	7	18	53	~(Mg _{0.75} Fe _{0.25}) ₂ SiO ₄
8			50	49	SiO ₂
9	16	1	30	52	(Mg,Fe)Si ₂ O ₃
10	22	2	24	52	(Mg,Fe)SiO ₃
11	6		38	55	MgSiO _x +SiO ₂
12	6		38	55	MgSiO _x +SiO ₂
13	22	10	18	50	~(Mg _{0.69} Fe _{0.31}) ₂ SiO ₄

valence of Fe^{2.5+}. Due to the use of the relatively thick sample, broadening of the spectrum as a result of the thickness effect was quite significant; however, the spectral quality is sufficient enough for us to conclude that the dominant state of the iron ions is Fe²⁺. Our modeled spectral fitting clearly reveals two intense doublets of the Fe²⁺ ions with the *QS* values of 2.68 (±0.06) and 1.65 (±0.06) mm/s at ambient conditions. This indicates the presence of two nonequivalent iron sites (Fe²⁺)₁ and (Fe²⁺)₂ in the ringwoodite structure. We also modeled the spectra with additional considerably weaker doublets, but could not find better reliable fits to the spectra than the two-doublet model. The *QS* values of the two doublets significantly increase with increasing pressure (Fig. 8), and can be represented by linear fits. The calculated parameters for (Fe²⁺)₁ and (Fe²⁺)₂ sites are: [*QS*(*P* = 0)]₁ = 2.68 ± 0.06 mm/s, *d*(*QS*)₁/*dP* = 0.0114 ± 0.0018 mm·s⁻¹·GPa⁻¹, and [*QS*(*P* = 0)]₂ = 1.65 ± 0.06 mm/s, *d*(*QS*)₂/*dP* = 0.0184 ± 0.0016 mm·s⁻¹·GPa⁻¹.

As pressure increases, significant changes in the spectra shape can be seen above 45 GPa (Fig. 7a). Starting from 35 GPa, an additional singlet-line component needs to be added to obtain the best fit to the spectra. The appearance of the singlet-line component reflects the disappearance of the quadrupole splitting of some iron ions, and is indicative of the transition of the high-spin

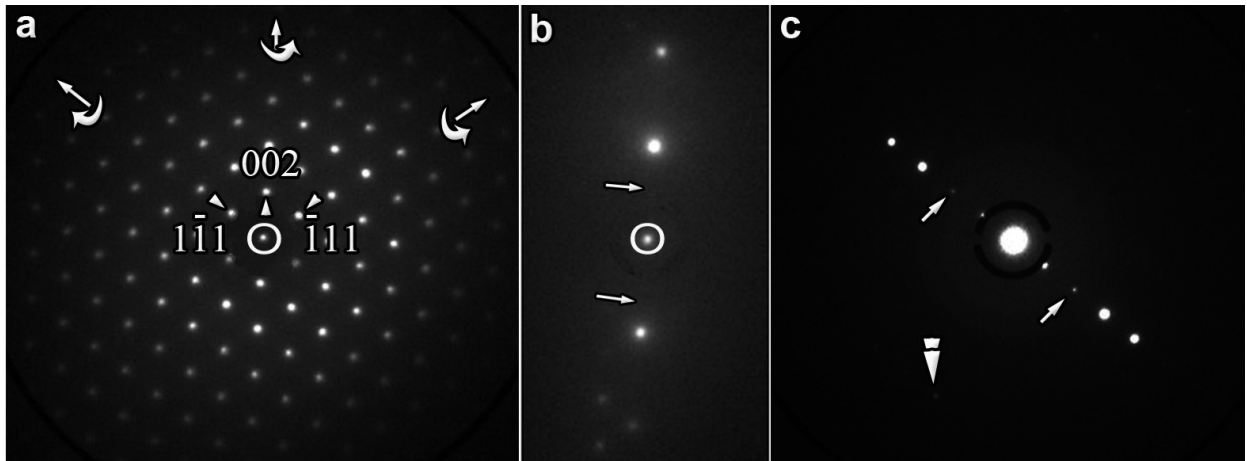


FIGURE 4. (a) Representative electron-diffraction patterns of ringwoodite [(Mg,Fe)₂SiO₄] obtained along B = [110] zone axis. Arrows show the axes around which the sample was rotated to determine the plural scattering effects. (b) The electron diffraction pattern from the sample rotated around the [001] axis. Forbidden reflections are shown by arrows. (c) The electron-diffraction pattern from the sample rotated around the [100] axis. The 222 reflections, demonstrated weak intensities due to the double diffraction (bigger arrows). The reflections responsible for double diffraction are shown by the smaller arrow.

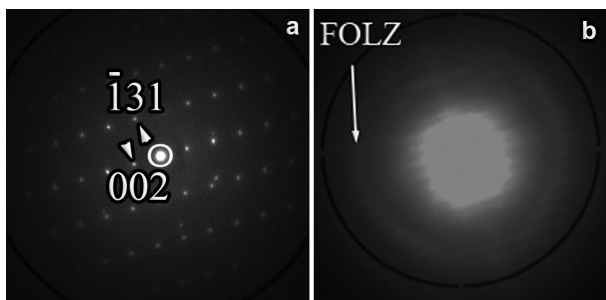


FIGURE 5. (a) The SAED pattern obtained in $B = [310]$ zone axis; (b) respective Kössel electron diffraction pattern demonstrating Kossel-type CBED pattern obtained at the same zone axis orientation as **a**. First-order Laue zone ring is shown.

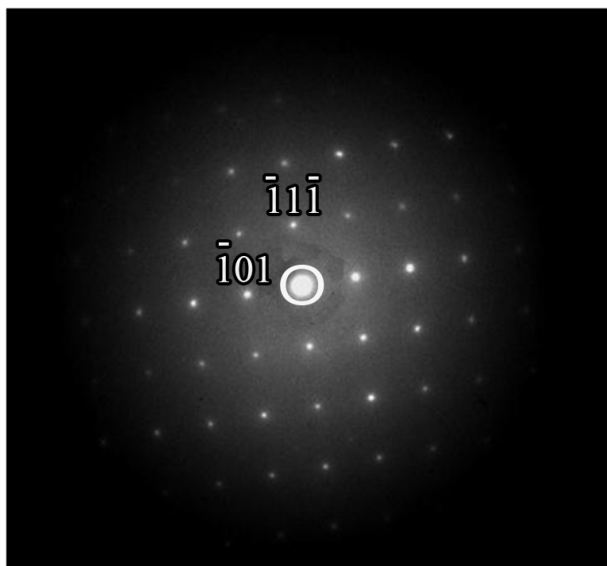


FIGURE 6. The SAED pattern from the MgSiO_3 grain obtained in $B = [121]$ zone axis.

(HS) ions Fe^{2+} with spin $S = 2$ into the low-spin (LS) state with $S = 0$ (Gutlich et al. 2011). With further pressure increase, the intensity of the singlet-line component increases at the expense of the doublet components up to 70 GPa. Above 70 GPa, the singlet-line component is the only remaining spectral feature of the Fe^{2+} ions, indicating the completion of the spin-pairing transition in both iron sites. SMS spectra recorded in the pressure release process (Fig. 7b) revealed that the HS-LS transition is reversible (Figs. 7, 8, and 9).

DISCUSSION

Ringwoodite, a spinel-structured solid solution in the $\text{Mg}_2\text{SiO}_4\text{-Fe}_2\text{SiO}_4$ series, is a high-pressure polymorph of olivine. As revealed by the electron diffraction patterns, our ringwoodite sample has a lattice parameter $a = 8.06 (\pm 0.1)$ Å in the space group $Fd\bar{3}m$ (Fig. 10). One can thus use Mössbauer spectroscopic analyses to assign iron sites (Fe^{2+}_1) and (Fe^{2+}_2) in the spinel structure. The $QS = 2.68$ mm/s of the predominant (Fe^{2+}_1) coincides very well with values reported in several previous papers for

$\gamma\text{-(Mg,Fe)}_2\text{SiO}_4$ ringwoodite (e.g., Choe et al. 1992; O'Neill et al. 1992, 1993; Taran et al. 2009; McCammon et al. 2004; Greenberg et al. 2011), and can be attributed to Fe^{2+} ions in the octahedral site (B-site) of the spinel structure. The (Fe^{2+}_2) component with $QS = 1.65$ mm/s can be attributed to Fe^{2+} ions in the tetrahedral sites (A-site) of the structure. In a stoichiometric ringwoodite with a nominal cation distribution $^{\text{VI}}[\text{Mg,Fe}]_2\text{ }^{\text{IV}}(\text{Si})\text{O}_4$, the presence of iron ions in the tetrahedral sites would lead to silicon redistribution from the tetrahedral to octahedral sites, $^{\text{VI}}[\text{Mg,Fe,Si}]_2\text{ }^{\text{IV}}(\text{Si,Fe})\text{O}_4$, producing the inverse or disordered ringwoodite structure. At ambient conditions, this is unlikely from the viewpoint of crystal chemistry due to the large difference in cationic radii between Si^{4+} and Fe^{2+} . However, at high pressures, the spinel structure may be slightly distorted with Si and Fe cations partially occupying both octahedral and tetrahedral sites (Hazen 1993). Indeed, Yagi et al. (1974) reported that about 2.3% of the total Si^{4+} cations may occupy the octahedral sites in ringwoodite. This type of partial cation disordering at high P - T in ferromagnesian silicate spinels was discussed and reviewed extensively by Hazen (1993), Hazen et al. (1993b), Hazen and Yang (1999), and O'Neill et al. (1992). A possible redistribution of Fe^{2+} between octahedral and tetrahedral sites in the inverse ringwoodite structure was also revealed in recent optical absorption spectral measurements (Taran et al. 2009).

Alternatively, the presence of the two Fe^{2+} doublets in our Mössbauer spectra may arise from differences in the next nearest neighbor environments in the octahedral site of the spinel structure. Both iron species (Fe^{2+}_1) and (Fe^{2+}_2) may reside in the octahedral site with slightly different local environments. This possibility was previously discussed for the perovskite iron silicates, in which differences in the local environments of the pseudo-dodecahedral site of Fe^{2+} result in doublets with different QS values (e.g., McCammon et al. 1992; Fei et al. 1994; McCammon 1997; Lauterbach et al. 2000). In addition, cation vacancies may appear (ordered or disordered) in the octahedral site of the spinel structure when hydrogen is present in hydrous ringwoodite (e.g., Inoue et al. 1995; Kohlstedt et al. 1996; Smyth et al. 2003; McCammon et al. 2004). It should also be noted that McCammon et al. (2004) observed a relatively weak Mössbauer absorption in $\gamma\text{-Fe}_2\text{SiO}_4$ ringwoodite with isomer shift $IS = 0.61$ mm/s and $QS = 0.85$ mm/s. They assigned these values to the charge transfer between Fe^{2+} and Fe^{3+}

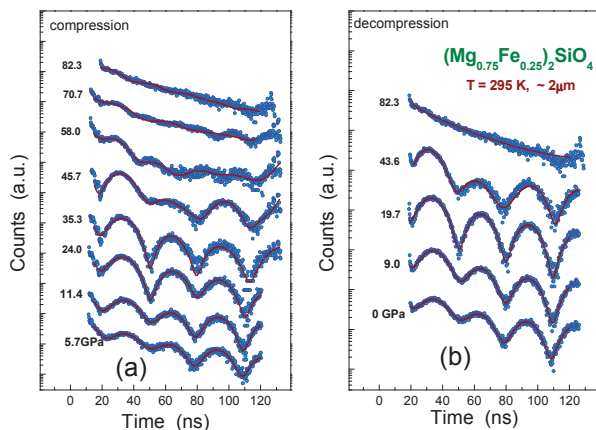


FIGURE 7. SMS spectra of ringwoodite $(\text{Mg}_{0.75}\text{Fe}_{0.25})_2\text{SiO}_4$ at high pressures and room temperature. (Color online.)

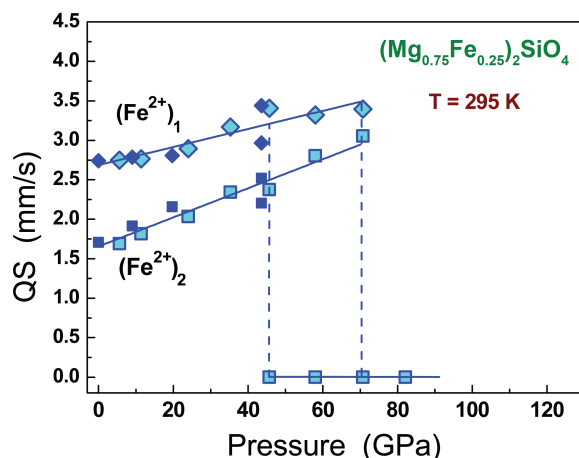


FIGURE 8. Quadrupole splitting (QS) of two iron sites in $(\text{Mg}_{0.75}\text{Fe}_{0.25})_2\text{SiO}_4$ ringwoodite at high pressures and room temperature. Open symbols; compression; solid symbols: decompression. (Color online.)

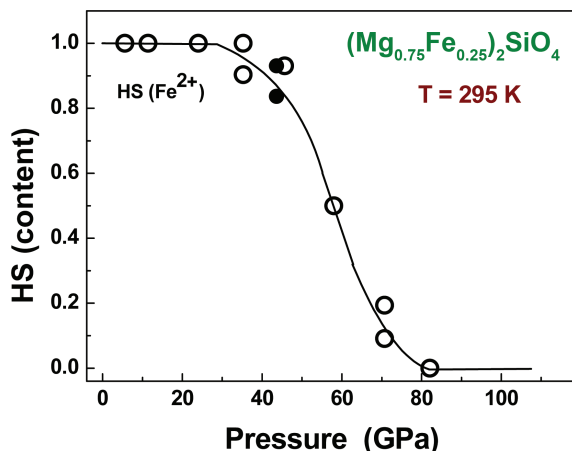


FIGURE 9. High-spin Fe^{2+} abundance as a function of pressure in $(\text{Mg}_{0.75}\text{Fe}_{0.25})_2\text{SiO}_4$ ringwoodite obtained from the SMS spectra at room temperature. (Color online.)

ions in adjacent octahedral sites of the ringwoodite structure.

Previous high-pressure Mössbauer measurements on the $\gamma\text{-Fe}_2\text{SiO}_4$ ringwoodite reported a linear decrease of the QS value with increasing pressure up to 16 GPa (Choe et al. 1992). This suggests that no electronic or polymorphic transitions occur up to 16 GPa, except for small and continuous changes of volume and local symmetry under pressure. On the basis of the crystal field calculations, the negative pressure derivative of QS was associated with a trend close to an ideal cubic symmetry of the oxygen sublattice (Choe et al. 1992). A similar decrease of QS was also found in $\gamma\text{-Fe}_2\text{SiO}_4$ at pressures up to 30 GPa (Greenberg et al. 2011).

Recent high-pressure X-ray diffraction and Mössbauer spectroscopy measurements on $\gamma\text{-Fe}_2\text{SiO}_4$ (Greenberg et al. 2011) also revealed a structural phase transition to a rhombohedrally distorted spinel phase at above 30 GPa. Two different Fe^{2+} crystallographic sites with an abundance ratio of $\text{Fe}_1:\text{Fe}_2 = 3:1$ were observed at pressures above 30 GPa. The ratio correlates with the distorted spinel structure in which Fe_1 is located in a distorted octahedron and Fe_2 is located in a symmetrical octahedron (Greenberg et al. 2011).

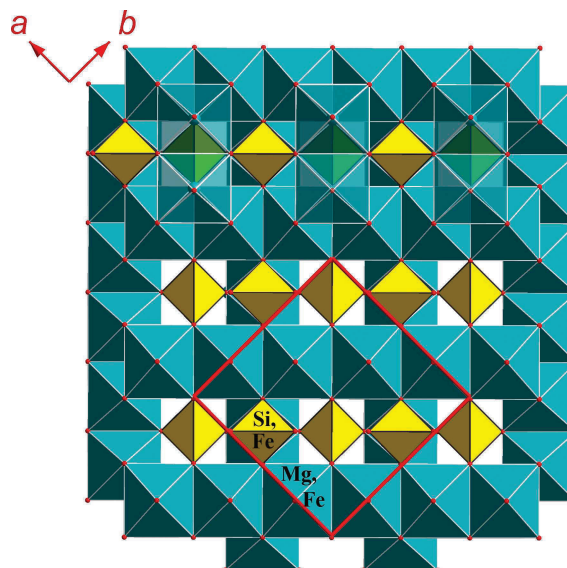


FIGURE 10. Crystal structure of ringwoodite. Representative Si, Fe, and Mg site occupations are shown to help understand the Mössbauer data interpretation. (Color online.)

At pressures above 30 GPa, the QS value in the Fe_2 symmetrical site increases, whereas the QS value in the Fe_1 distorted site continues to decrease. However, no spin transition was observed up to 61 GPa (Greenberg et al. 2011). The high-pressure behavior of the QS in our sample is quite different from this previous report, though. With increasing pressure, the QS values increase in both iron sites, and the high-spin to low-spin transition clearly occurs in both sites. At room temperature, the spin transition is continuous, reversible, and occurs in the region of 45–70 GPa (Figs. 7 and 8). These differences may be a result of the compositional variation in which Fe-rich $\gamma\text{-Fe}_2\text{SiO}_4$ helps stabilize the high-spin state.

It should be noted that most of the high-pressure Mössbauer measurements were conducted on $\gamma\text{-Fe}_2\text{SiO}_4$, an end-member in the ringwoodite system (Greenberg et al. 2011; Choe et al. 1992), and that the HS-LS spin crossover was not observed at pressures below 61 GPa (Greenberg et al. 2011). On the other hand, a spin crossover of Fe^{2+} at pressures between approximately 40 and 75 GPa was recently observed in olivine with composition $(\text{Mg}_{0.9}\text{Fe}_{0.1})_2\text{SiO}_4$ (Rouquette et al. 2008). However, the QS values are quite different in olivine and ringwoodite. Our findings here indicate that the electronic structures of ringwoodite at high pressures strongly depend on the ratio of Mg and Fe ions in the sample $(\text{Mg}_{1-x}\text{Fe}_x)_2\text{SiO}_4$.

ACKNOWLEDGMENTS

This work is supported by the Russian Foundation for Basic Research grants no. 11-02-00636, 12-05-31342, 11-02-00291, by RAS Program “Elementary particle physics, fundamental nuclear physics and nuclear technologies,” by the Russian Ministry of Education and Science Grant no. 16.518.11.7021, and by the Council on Grants of the President of the Russian Federation for the Support of Leading Scientific Schools (project no. NSh-2883.2012.5). This work at University of Texas Austin was supported by the U.S. National Science Foundation (EAR-0838221 and EAR-1053446) and the Carnegie/DOE Alliance Center. The support from the DOE Grant DE-FG02-02ER45955 for the work at GL and at the APS synchrotron facility is greatly acknowledged. Synchrotron Mössbauer experiments were performed at HPCAT (Sector 16), APS, ANL. HPCAT is supported by DOE-BES, DOE-NNSA, NSF, and the W.M. Keck Foundation. APS is supported by DOE-BES, under Contract no. DE-AC02-06CH11357.

REFERENCES CITED

- Akimoto, S., and Ida, Y. (1966) High-pressure synthesis of Mg₂SiO₄. *Earth and Planetary Science Letters*, 1, 358–359.
- Angel, R.J., Chopelas, A., and Ross, N.L. (1992) Stability of high-density clinoenstatite at upper-mantle pressures. *Nature*, 358, 322–324.
- Choe, I., Ingalls, R., Brown, J.M., and Sato-Sorensen, Y. (1992) Mossbauer studies of iron silicate spinel at high pressure. *Physics and Chemistry of Minerals*, 19, 236–239.
- Fei, Y., and Bertka, C.M. (1999) Phase transitions in the Earth's mantle and mantle mineralogy. *The Geochemical Society Special Publications*, 6, 189–207.
- Fei, Y., Virgo, D., Mysen, B.O., Wang, Y., and Mao, H.K. (1994) Temperature-dependent electron delocalization in (Mg,Fe)SiO₃ perovskite. *American Mineralogist*, 79, 826–837.
- Frost, D.J. (2008) The upper mantle and transition zone. *Elements*, 4, 171–176.
- Gavriluk, A.G., Lin, J.F., Lyubutin, I.S., and Struzhkin, V.V. (2006) Optimization of the synchrotron mossbauer experiment for high-pressure studies of electronic transitions: Magnesioiwustite (Mg, Fe)O. *JETP Letters*, 84, 161–166.
- Greenberg, E., Dubrovinsky, L.S., McCammon, C., Rouquette, J., Kantor, I., Prakapenka, V., Rozenberg, G. Kh., and Pasternak, M.P. (2011) Pressure-induced structural phase transition of the iron end-member of ringwoodite (γ -Fe₂SiO₄) investigated by X-ray diffraction and Mössbauer spectroscopy. *American Mineralogist*, 96, 833–840.
- Gutlich, P., Bill, E., and Trautwein, A.X. (2011) Electric quadrupole interaction. In P. Gutlich, E. Bill, and A.X. Trautwein, Eds., *Mössbauer Spectroscopy and Transition Metal Chemistry*, 89–100. Springer-Verlag, Berlin.
- Hahn, Th. (2006) *International Tables for Crystallography*, Vol. A: space-group symmetry, 696–703. Springer, Berlin.
- Hazen, R.M. (1993) Comparative crystal chemistry of silicate spinels: Anomalous behavior of (Mg,Fe)₂SiO₄. *Science*, 259, 206–209.
- Hazen, R.M., and Yang, H. (1999) Effect of cation distribution and order disorder on P-V-T equations of states of cubic spinels. *American Mineralogist*, 84, 1956–1960.
- Hazen, R.M., Downs, R.T., Finger, L.W., and Ko, J. (1993) Crystal chemistry of ferromagnesian silicate spinels: Evidence for Mg-Si disorder. *American Mineralogist*, 78, 1320–1323.
- Inoue, T., Yurimoto, H., and Kudoh, Y. (1995) Hydrous modified spinel Mg_{1.75}Si_{0.5}O₄: A new water reservoir in the mantle transition region. *Geophysical Research Letters*, 22, 117–120.
- Irifune, T., Shinmei, T., McCammon, C.A., Miyajima, N., Rubie, D.C., and Frost, D.J. (2010) Iron partitioning and density changes of pyrolite in Earth's lower mantle. *Science*, 327, 193–195.
- Koch, M., Woodland, A.B., and Angel, R.J. (2004) Stability of spinelloid phases in the system Mg₂SiO₄-Fe₂SiO₄-Fe₃O₄ at 1100 °C and up to 10.5 GPa. *Physics of the Earth and Planetary Interiors*, 143, 171–183.
- Koch-Müller, M., Rhede, D., Schulz, R., and Wirth, R. (2009) Breakdown of hydrous ringwoodite to pyroxene and spinelloid at high P and T and oxidizing conditions. *Physics and Chemistry of Minerals*, 36, 329–341.
- Kohlstedt, D.L., Keppler, H., and Rubie, D.C. (1996) The solubility of water in α , β and γ phases of (Mg,Fe)₂SiO₄. *Contributions to Mineralogy and Petrology*, 123, 345–357.
- Lauterbach, S., McCammon, C.A., van Aken, P., Langenhorst, F., and Seifert, F. (2000) Mossbauer and ELNES spectroscopy of (Mg,Fe)(Si,Al)O₃ perovskite: A highly oxidised component of the lower mantle. *Contributions to Mineralogy and Petrology*, 138, 17–26.
- Lin, J.F., and Tsuchiya, F. (1999) Spin transition of iron in the Earth's lower mantle. *Physics of the Earth and Planetary Interiors*, 170, 248–259.
- Lin, J.F., Vankó, G., Jacobsen, S.D., Iota, V., Struzhkin, V., Prakapenka, V.B., Kuznetsov, A., and Yoo, C.S. (2007) Spin transition zone in Earth's lower mantle. *Science*, 317, 1740–1743.
- Lyubutin, I.S., Gavriluk, A.G., Frolov, K.V., Lin, J.F., and Trojan, I.A. (2009) High-spin-low-spin transition in magnesioiwustite (Mg_{0.75}Fe_{0.25})O at high pressures under hydrostatic conditions. *JETP Letters*, 90, 617–622.
- Lyubutin, I.S., Struzhkin, V.V., Mironovich, A.A., Gavriluk, A.G., Naumov, P.G., Lin, J.F., Ovchinnikov, S.G., Sinogeikin, S., Chow, P., and Xiao, Y. (2013) Quantum critical point and spin fluctuations in the lower-mantle ferropericlase. *Proceedings of the National Academy of Sciences*, 110, 7142–7147.
- Mao, H.K., Bell, P.M., Shaner, J.W., and Steinberg, D.J. (1978) Specific volume measurements of Cu, Mo, Pd, and Ag and calibration of the ruby R1 fluorescence pressure gauge from 0.06 to 1 Mbar. *Journal of Applied Physics*, 49, 3276–3283.
- Mao, Z., Lin, J.F., Liu, J., and Prakapenka, V.B. (2011) Thermal equation of state of lower-mantle ferropericlase across the spin crossover. *Geophysical Research Letters*, 38, L23308.
- McCammon, C. (1997) Perovskite as a possible sink for ferric iron in the lower mantle. *Nature*, 387, 694–696.
- (2006) Microscopic properties to macroscopic behavior: The influence of iron electronic states. *Journal of Mineralogical and Petrological Sciences*, 101, 130–144.
- McCammon, C.A., Rubie, D.C., Ross, C.R. II, Seifert, F., and O'Neill, H.St.C. (1992) Mossbauer spectra of 57Fe_{0.05}Mg_{0.95}SiO₃ perovskite at 80 and 298 K. *American Mineralogist*, 77, 894–897.
- McCammon, C.A., Frost, D.J., Smyth, J.R., Laustsen, H.M.S., Kawamoto, T., Ross, N.L., and van Aken, P.A. (2004) Oxidation state of iron in hydrous mantle phases: Implications for subduction and mantle oxygen fugacity. *Physics of the Earth and Planetary Interiors*, 143–144, 157–169.
- Morishima, H., Kato, T., Suto, M., Ohtani, E., Urakawa, S., Utsumi, W., Shimomura, O., and Kikegawa, T. (1994) The phase boundary between α - and β -Mg₂SiO₄ determined by in situ X-ray observation. *Science*, 265, 1202–1203.
- Murakami, T., Takeuchi, Y., and Yamanaka, T. (1984) X-ray studies on protoenstatite II. Effect of temperature on the structure up to near the incongruent melting point. *Zeitschrift für Kristallographie*, 166, 263–275.
- O'Keefe, M., Hyde, B.G., and Bovin, J.O. (1979) Contribution to the crystal chemistry of orthorhombic perovskites: MgSiO₃ and NaMgF₃. *Physics and Chemistry of Minerals*, 4, 299–305.
- O'Neill, H. St.C., Annersten, H., and Vargo, D. (1992) The temperature dependence of the cation distribution in magnesioferrite (MgFe₂O₄) from powder XRD structural refinements and Mössbauer spectroscopy. *American Mineralogist*, 77, 725–740.
- O'Neill, H. St.C., McCammon, C.A., Canil, D., Rubie, D.C., Ross, C.R. II, and Seifert, H.F. (1993) Mössbauer spectroscopy of mantle transition zone phases and determination of minimum Fe³⁺ content. *American Mineralogist*, 78, 456–460.
- Ohtani, E. (1979) Melting relation of Fe₂SiO₄ up to about 200 kbar. *Journal of Physics of the Earth*, 27, 189–208.
- Ringwood, A.E., and Major, A. (1966) Synthesis of Mg₂SiO₄-Fe₂SiO₄ spinel solid solutions. *Earth and Planetary Science Letters*, 1, 241–245.
- Rouquette, J., Kantor, I., McCammon, C.A., Dmitriev, V., and Dubrovinsky, L.S. (2008) High-pressure studies of (Mg_{0.95}Fe_{0.1})₂SiO₄ olivine using raman spectroscopy, X-ray diffraction, and Mössbauer spectroscopy. *Inorganic Chemistry*, 47, 2668–2673.
- Sasaki, S., Takeuchi, Y., Fujino, K., and Akimoto, S. (1982) Electron-density distributions of three orthopyroxenes: Mg₂Si₂O₆, Co₂Si₂O₆, and Fe₂Si₂O₆. *Zeitschrift für Kristallographie*, 158, 279–297.
- Shvyd'ko, Yu.V. (1999) Nuclear resonant forward scattering of X-rays: Time and space picture. *Physical Review B*, 59, 9132–9143.
- Shvyd'ko, Yu.V., Lerche, M., Jäschke, J., Lucht, M., Gerdau, E., Gerken, M., Rüter, H.D., Wille, H.-C., Becker, P., Alp, E.E., Sturhahn, W., Sutter, J., and Toellner, T.S. (2000) γ -ray wavelength standard for atomic scales. *Physical Review Letters*, 85, 495–498.
- Smirnov, G.V. (1999) General properties of nuclear resonant scattering. *Hyperfine Interactions*, 123–124, 31–77.
- Smyth, J.R., Holl, C.M., Frost, D.J., Jacobsen, S.D., Langenhorst, F., and McCammon, C.A. (2003) Structural systematics of hydrous ringwoodite and water in Earth's interior. *American Mineralogist*, 88, 1402–1407.
- Suito, K. (1972) Phase transformations of pure Mg₂SiO₄ into a spinel structure under high pressures and temperatures. *Journal of Physics of the Earth*, 20, 225–243.
- Taran, M.N., Koch-Müller, M., Wirth, R., Abs-Wurmbach, I., Rhede, D., and Greshake, A. (2009) Spectroscopic studies of synthetic and natural ringwoodite, γ -(Mg, Fe)₂SiO₄. *Physics and Chemistry of Minerals*, 36, 217–232.
- van Aken, P.A., and Woodland, A.B. (2006) Crystal chemistry of spinel and spinelloid solid solutions in the system Fe₂SiO₄-Fe₃O₄. *Geophysical Research Abstracts*, 8, 07770. European Geosciences Union.
- Woodland, A.B., and Angel, R.J. (1998) Crystal structure of a new spinelloid with the wadsleyite structure in the system Fe₂SiO₄-Fe₃O₄ and implications for the Earth's mantle. *American Mineralogist*, 83, 404–408.
- Yagi, T., Marumo, F., and Akimoto, S. (1974) Crystal structures of spinel polymorphs of Fe₂SiO₄ and Ni₂SiO₄. *American Mineralogist*, 59, 486–490.
- Yamanaka, T., Tobe, H., Shimazu, T., Nakatsuka, A., Dobuchi, Y., Ohtaka, O., Nagai, T., and Ito, E. (1998) Phase relations and physical properties of Fe₂SiO₄-Fe₃O₄ solid solution under pressures up to 12 GPa. In M. Manghni and T. Yogi, Eds., *Properties of earth and planetary materials at high pressure and temperature*, 457–459. Geophysical Monograph, American Geophysical Union, Washington, D.C.
- Yamanaka, T., Shimazu, H., and Ota, K. (2001) Electric conductivity of Fe₂SiO₄-Fe₃O₄ spinel solid solutions. *Physics and Chemistry of Minerals*, 28, 110–118.

MANUSCRIPT RECEIVED NOVEMBER 10, 2012

MANUSCRIPT ACCEPTED JUNE 9, 2013

MANUSCRIPT HANDLED BY SERGIO SPEZIALE